

UV-cured self-replenishing hydrophobic polymer films

Citation for published version (APA):

Zhang, Y., Rocco, C., Karasu, F., Ven, van der, L. G. J., Benthem, van, R. A. T. M., Allonas, X., Croutxé-Barghorn, C., Esteves, A. C. C., & With, de, G. (2015). UV-cured self-replenishing hydrophobic polymer films. *Polymer*, 69, 384-393. <https://doi.org/10.1016/j.polymer.2015.02.036>

Document license:

TAVERNE

DOI:

[10.1016/j.polymer.2015.02.036](https://doi.org/10.1016/j.polymer.2015.02.036)

Document status and date:

Published: 01/01/2015

Document Version:

Publisher's PDF, also known as Version of Record (includes final page, issue and volume numbers)

Please check the document version of this publication:

- A submitted manuscript is the version of the article upon submission and before peer-review. There can be important differences between the submitted version and the official published version of record. People interested in the research are advised to contact the author for the final version of the publication, or visit the DOI to the publisher's website.
- The final author version and the galley proof are versions of the publication after peer review.
- The final published version features the final layout of the paper including the volume, issue and page numbers.

[Link to publication](#)

General rights

Copyright and moral rights for the publications made accessible in the public portal are retained by the authors and/or other copyright owners and it is a condition of accessing publications that users recognise and abide by the legal requirements associated with these rights.

- Users may download and print one copy of any publication from the public portal for the purpose of private study or research.
- You may not further distribute the material or use it for any profit-making activity or commercial gain
- You may freely distribute the URL identifying the publication in the public portal.

If the publication is distributed under the terms of Article 25fa of the Dutch Copyright Act, indicated by the "Taverne" license above, please follow below link for the End User Agreement:

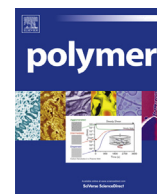
www.tue.nl/taverne

Take down policy

If you believe that this document breaches copyright please contact us at:

openaccess@tue.nl

providing details and we will investigate your claim.



UV-cured self-replenishing hydrophobic polymer films



Y. Zhang^a, C. Rocco^b, F. Karasu^b, L.G.J. van der Ven^{a,c}, R.A.T.M. van Benthem^{a,d},
X. Allonas^b, C. Croutxé-Barghorn^b, A.C.C. Esteves^{a,*}, G. de With^{a,*}

^a Laboratory of Materials and Interface Chemistry, Department of Chemical Engineering and Chemistry, Eindhoven University of Technology, Den Dolech 2, 5612AZ Eindhoven, The Netherlands

^b Laboratory of Macromolecular Photochemistry and Engineering, University of Haute Alsace, ENSCMu, 3 Rue Alfred Werner, 68093 Mulhouse, France

^c AkzoNobel, Automotive & Aerospace Coatings, P. O. Box 3, 2170BA Sassenheim, The Netherlands

^d DSM Ahead BV Netherlands, P. O. Box 18, 6160MD Geleen, The Netherlands

ARTICLE INFO

Article history:

Received 5 December 2014

Received in revised form

18 February 2015

Accepted 19 February 2015

Available online 26 February 2015

Keywords:

Self-replenishing

Hydrophobic

UV-curing

ABSTRACT

Self-healing functional polymer surfaces, designed with an intrinsic and spontaneous mechanism which replenishes the damaged surfaces with the original chemical functionalities, are of great interest to maintain a high performance of the functionality and extend the life-time of materials.

We report self-replenishing UV-cured hydrophobic polymer films prepared through the incorporation of methacrylate-terminated perfluorinated-dangling chains into poly(ethylene glycol diacrylate) (PEGDA)-based networks. The films are able to spontaneously and fully self-replenish the surface hydrophobicity, multiple times, upon consecutive intentional damages. The rate of recovery was found to be dependent on the glass transition temperature (T_g) of the networks, which directly correlates to the PEG block length in the PEGDA oligomer used. This study demonstrates that an intrinsic self-replenishing mechanism can be implemented in new network architectures, created rapidly and efficiently by free radical UV-polymerization, which allows preparing self-healing functional polymer films in a faster and eco-friendlier way.

© 2015 Elsevier Ltd. All rights reserved.

1. Introduction

Low surface energy polymeric films are widely used in industrial applications exploring their advantageous properties such as hydrophobicity, easy-to-clean or anti-fouling behavior. In order to achieve these desired surface properties, films have been modified by surface treatments such as plasma irradiation [1,2], chemical grafting [3–6] or using copolymers containing hydrophobic blocks [7–13]. Another extensively applied strategy is self-stratification, realized by blending with small amounts of low surface energy additives which are able to segregate towards the surface during film formation [14–17]. Several research groups have investigated the effect of end-functionalized polymeric additives on the surface composition and properties of different model systems [18–22]. The molecular weight and the molecular architecture are perceived as the most influential factors on the surface segregation behavior.

Generally, these strategies for tailoring the surface properties are efficient and have little impact on the bulk properties of the polymeric films. However, once surface damage occurs the properties dependent on the surface chemical composition (and/or topography) will be lost due to the loss of the surface functional groups. Hence, introducing a self-healing mechanism in such functional polymeric films will be highly advantageous for keeping a high performance of the surface functionalities during an extended service-life.

The self-healing materials concept has received wide interest both from academia and industry in the last two decades [23–25]. For polymers and polymer films, most of the self-healing strategies aim at repairing mechanical properties or material integrity, for which several approaches have been reported, namely encapsulation [26,27], reversible bonds/interactions [28–31] or deformation recovery [32]. Much less attention has been paid to self-healing mechanisms aiming to recover surface functionalities. Recently, we reported a functionality self-repairing concept based on self-replenishing surfaces, through the surface segregation of functional groups connected to a polymeric network [33] driven by energy differences between surface and bulk. The concept was

* Corresponding authors.

E-mail addresses: a.c.c.esteves@tue.nl (A.C.C. Esteves), G.deWith@tue.nl (G. de With).

proven for model systems, consisting of thermally cross-linked polycaprolactone (PCL)-based films containing perfluoroalkyl-polymeric dangling chains, which are able to self-reorient towards the air-polymer interfaces created upon damage, so that the surface properties are spontaneously repaired (Fig. 1).

One of the main requisites for self-healing materials is sufficient mobility of the “healing” components or of a part (phase) of the system. For self-replenishing polymer films, a well-tuned polymer chain mobility [34,35] and proper surface energy differences [36] have been reported to be crucial. In the model systems, a PCL-based polymeric spacer was used to enhance the miscibility of the low surface energy fluorinated dangling chains with the network-binder providing enough mobility for the self-segregation of the dangling chains.

For specific surface properties, like superhydrophobicity, the functionality is not only dependent on the surface chemical composition but also on topography. In these cases, the self-repairing mechanism should provide the recovery of the chemical composition while the topography is simultaneously reproduced or reconstructed. Accordingly, the self-replenishing mechanism has also been reported on surface-structured polymeric films containing silica nanoparticles of two different size distributions [36,37]. The chemical composition is repaired by the surface segregation mechanism described above and a surface topography is recreated by the damage, via the silica nanoparticles covalently bonded to the polymer network and homogeneously distributed throughout the bulk of the polymer film. Other authors used similar self-segregating or self-orientation principles on rough or porous surfaces to develop self-healing functional surfaces. Li et al. [38] and Jin et al. [39] reported self-healing superhydrophobic materials based on surfactant-coated porous surfaces and structured materials, Lin and coworkers [40,41] developed a self-healing superhydrophobic polymer-coated cotton and Kuroki et al. [42] reported self-healing anti-fouling polymer films.

The simplicity and versatility of the self-replenishing concept makes it very attractive for industrial applications, especially in coatings. However, the low hardness and poor mechanical properties of the model chemical systems studied so far, and the time- and energy-consuming preparation methods reported, namely thermal curing, are still hindering practical applications. Nowadays, photocurable polymeric materials are attracting a renewed industrial and academic interest in the field of polymer coatings due to its fast curing, eco-friendliness and excellent performance [43,44] characteristics. Hence, using UV-curing instead of thermal curing to obtain self-healing/self-replenishing polymer films could improve significantly the curing speed and readily allow exploring systems with better thermal and mechanical properties by tuning the network architecture. This implementation could, however, have strong implications on the self-healing ability of the polymer films, for example if the mobility or the miscibility of the “healing” agents (i.e., dangling chains) is somehow compromised by the fast photo-curing process. Gan et al. [45] reported photopolymerized acrylate-based systems containing fluorinated copolymers as additives, which self-segregate towards the air-interface to form self-wrinkled patterns. These systems already hint for a self-replenishing ability, but the surface characteristics were not fully recovered and needed to be triggered by heating the damaged films at 130 °C for 30 min.

In this paper, we investigated the self-replenishing capability of new hydrophobic cross-linked polymer films prepared by UV-initiated polymerization. Acrylate-based polymer networks were chosen due to their well-known high reactivity and wide choice of monomers available [46]. The polymer networks were built up with poly(ethyleneglycol diacrylates) (PEGDA) of variable length while the dangling chains consisted of fluorinated-polymeric spacers designed with terminal methacrylate group, which is preferentially co-reacted with the acrylic groups upon UV-initiated radical polymerization. The influence of the oligo-ethyleneglycol network polymer segment length on the hydrophobicity and self-replenishing efficiency of the polymer films is discussed.

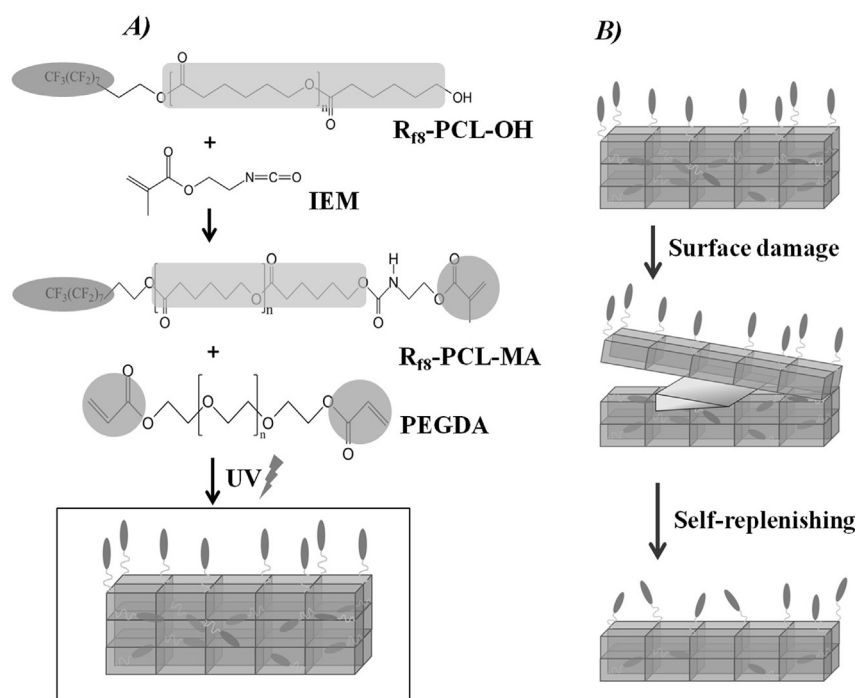


Fig. 1. Chemical components and scheme of self-replenishing films prepared: A) chemical synthesis route of the methacrylate-terminated dangling chains ($R_{18}\text{-PCL-MA}$) and the schematic representation of the UV-cured polymer network with dangling chains; B) schematic of the self-replenishing mechanism via the re-orientation of dangling chains towards the new air-coating film interfaces created upon the surface damage.

2. Experimental

2.1. Materials

PEGDA of different molecular weights ($M_n = 200$ (4 units of EG), 400 (9 units of EG) and 600 (13 units of EG) g/mol, denoted as PEG200DA, PEG400DA and PEG600DA, respectively) were kindly offered by Sartomer (with the commercial names of SR259, SR344 and SR610, respectively). 2-isocyanatoethyl methacrylate (IEM, purity 98%) and dibutyltin dilaurate (DBTDL, purity 95%) were purchased from Sigma–Aldrich. The radical photoinitiator Darocur 1173 (purity 99%) was kindly offered by BASF. All the solvents were purchased from Biosolve bv and used as received, unless stated otherwise.

2.2. Synthesis and characterization of the fluorinated-polymeric dangling chains terminated with a methacrylate group (R_{f8} -PCL₁₆-MA)

The synthesis of the methacrylate-terminated dangling chains consisted of two steps. The first was the preparation of the fluorinated-polymeric dangling chains terminated with a hydroxyl group, (R_{f8} -PCL₁₆-OH, Fig. 1A) by ring opening polymerization, as previously described [47]. The second step was to introduce the UV cross-linkable methacrylate group using IEM, via the chemical modification of the R_{f8} -PCL₁₆-OH dangling chains. A typical procedure for the reaction was as follows: a solution of R_{f8} -PCL₁₆-OH (14.2 g, 6.06 mmol) and DBTDL catalyst (38.3 mg, 6.06×10^{-2} mmol) in 20 ml dried tetrahydrofuran (THF) was prepared in a well dried and nitrogen purged flask, equipped with a magnetic stirrer. After stirring and heating the solution to 50 °C with an oil bath, IEM (1.035 g, 6.67 mmol) was added into the flask drop-wise via syringe. The overall NCO/OH ratio was set as 1.1/1 to ensure full conversion of the hydroxyl groups. After 24 h of reaction at 50 °C under a nitrogen atmosphere, the reaction product was diluted with THF and precipitated in *n*-heptane. These dissolving-precipitation steps were repeated twice for the purpose of purification. A white powder (R_{f8} -PCL₁₆-MA, Fig. 1A) was finally obtained after removal of the solvents and drying under vacuum. After the purification, the reaction yield was 88% based on the mass of the collected product.

The chemical structure of the synthesized material was characterized by ¹H NMR, carried out on a Varian 400 spectrometer at 25 °C, operating at 400 MHz. Deuterated acetone (with TMS as internal standard) was used as solvent. The number average molecular weight (M_n) and polydispersity index (PDI) were obtained by Gel Permeation Chromatography (GPC), using a Waters GPC equipped with Waters model 510 pump and a model 410 differential refractometer. A set of two mixed bed columns (Mixed-C, Polymer Laboratories, 30 cm, 40 °C) was used and THF was selected as eluent. The system was calibrated using narrow molecular weight polystyrene standards ranging from 600 to 7×10^6 g/mol. The conversion of the isocyanate groups before and after the reaction, was followed by Fourier Transform-Infrared (FT-IR) Attenuated Total Reflectance (ATR) Spectroscopy performed on a Varian 3100 FT-IR spectrometer with DTGS detector. The measurements were conducted by applying a drop of the reaction mixture in THF on the ATR diamond unit at ambient conditions. Each spectrum was obtained from an average of 50 scans collected with a resolution of 4 cm⁻¹. The vibration band at 1740 cm⁻¹, assigned to the stretching of the C=O group of the isocyanate functionality, was used as internal reference. Additional MALDI ToF MS and ¹³C NMR analyses of the R_{f8} -PCL₁₆-OH and R_{f8} -PCL₁₆-MA dangling chains is provided in the Supporting information (SI), Figures S1 and S2.

2.3. Preparation and characterization of the UV-cured polymer films

Several cross-linked polymer films were prepared from mixtures of PEGDA oligomer (binder), R_{f8} -PCL₁₆-MA and radical photoinitiator (PI) (Table 1). Due to the low miscibility between the oligomers and the dangling chains, 1,4-dioxane, a good solvent for both oligomers and dangling chains, was added to the mixtures, which all appeared as transparent solutions. These solutions were casted on glass substrates (previously cleaned with acetone and dried in an oven) by a doctor blade applicator (with an approximate wet thickness of 120 μm) and then cured for 30 s under UV irradiation, inside a N₂-filled quartz chamber. The UV lamp (high pressure mercury lamp, Dr. Hönle AG) power was 142 mW/cm² with UVV 50 mW/cm², UVA 69 mW/cm², UVB 23 mW/cm² and UVC 0 mW/cm², as measured by UV Power Puck, while the thickness of the films after curing was typically 30–50 μm.

The thermal properties of the UV-cured films were studied by Thermogravimetric Analyses (TGA) and Differential Scanning Calorimetry (DSC). For TGA, samples with a mass ranging from 5 to 10 mg were analyzed on a TA Q500 instrument. The temperature was increased linearly from RT to +600 °C, at a rate of 10 °C/min under a nitrogen flow. DSC measurements were conducted on a TA Q2000 instrument. Samples with a mass of 6–8 mg were analyzed with the following procedure: equilibration at +20 °C; heating to +150 °C at 10 °C/min; isothermal at +150 °C for 3 min; cooling to –60 °C at 10 °C/min; isothermal at –60 °C for 3 min and finally heating to +150 °C at 10 °C/min. The first cooling and second heating runs were selected for the analyses of the results. DMA measurements were attempted but it was not possible to prepare robust films, with sufficient thickness and size-dimensions to be held firmly in the equipment.

The amount of unreacted species remaining in the UV-cured films was evaluated by solvent extraction experiments. The films were first vacuum dried in the oven at +40 °C until their mass remained constant. Next, the films were immersed in selected solvents (chloroform or deionized water) for 30 min, followed by sonication during 15 min (in a sonication bath). After the polymer films and solvents were separated, the solvents were evaporated to collect the solid extractable residues. Both extractable solid residues and polymer films were vacuum dried in oven at +20 °C for 24 h and +60 °C for 4 h. The weight loss corresponding to the extraction of the non-reacted (and/or non-bonded) species was calculated using Equation (1) where M_{original} and $M_{\text{extractable}}$ represent the mass of the original film and the mass of the extractable residues, respectively.

$$\text{Weight loss \%} = \frac{M_{\text{extractable}}}{M_{\text{original}}} \times 100\% \quad (1)$$

Table 1

Chemical components and concentrations used in the preparation of the UV-cured polymer films.

	Nomenclature	R_{f8} -PCL ₁₆ -MA (wt %)	Binder (wt%)	Photoinitiator (wt%)	Dioxane (wt%)	Overall F content (wt%) ^a
1	PEG200DA	–	99	1	–	0
2	PEG400DA	–	99	1	–	0
3	PEG600DA	–	99	1	–	0
4	PEG200DA-F	7.8	71.2	1	20	1.5
5	PEG400DA-F	7.8	71.2	1	20	1.5
6	PEG600DA-F	7.8	71.2	1	20	1.5

^a In relation to the total solid contents of the film (monomer + PI + dangling chain).

The conversion of the vinyl groups upon UV irradiation throughout the depth of the polymer films was studied by Confocal Raman microscopy (CRM). The Raman spectra were recorded with a Jobin Yvon (Horiba) spectrometer using a HeNe laser at a wavelength of 632 nm and controlled by a motorized stage. CRM depth profiling was performed in air, thus the focus was slightly shifted due to refraction of the transparent polymer films [48]. 100 × magnification objectives (Olympus) with a 400-μm pinhole were used and a laser step increment of 3 μm was set for CRM depth profiling. The band at 1640 cm⁻¹, attributed to the stretching vibration of the vinyl bonds was selected to follow the monomer conversion. The band at 1716 cm⁻¹, attributed to the stretching vibration of the C=O groups was used as the internal reference. The chemical conversion was estimated based on Equation (2), where A_0 denotes the area of the band at time zero (liquid mixture) and A_t is the area of the band at a determined time t .

$$\text{Conversion \%} = \left[1 - \left(\frac{A_t(1640)}{A_t(1716)} \right) / \left(\frac{A_0(1640)}{A_0(1716)} \right) \right] \times 100 \quad (2)$$

The hydrophobicity of the polymer films was evaluated by dynamic water contact angles (CA) measured with a Data Physics OCA 30 instrument. Advancing (CA_{adv}) and receding (CA_{rec}) water contact angles were measured with the ARCA-software mode and the following procedure: A 0.2 μL droplet was first placed on the surface; further water was injected into the droplet up to 15 μL at the speed of 0.5 μL/s; after a waiting period of 2 s, the water was retracted from the droplet until 2 μL at 0.5 μL/s. The CA_{adv} was calculated when the droplet base diameter was increasing linearly, while the CA_{rec} was calculated when the droplet base diameter was decreasing linearly. The errors provided correspond to the standard deviation of the sample; three to five different surface regions were measured.

The chemical composition of the top-surface of the UV-cured films was investigated by X-ray photoelectron spectroscopy (XPS), carried out with a K-Alpha, ThermoScientific spectrometer using an aluminum anode (Al Kα = 1486.3 eV) and operating at 510 W with a background pressure of 8×10^{-8} mbar. The spectra were recorded using a VGX900 data system and collecting an average of 30 scans for each measurement. The spectra were acquired at take-off angle of 0° relative to the surface normal, corresponding to a probe depth of about 10 nm. The errors provided correspond to the standard deviation of the sample; four different surface regions were measured. The Fluorine/Carbon (F/C) atomic ratio was determined from curves fitted to the C 1s peak from the carbon environment (C–C, C–H, C–O, C–N, C=O, C–F₂ and C–F₃) and the F 1s peak. The areas were corrected for the element sensitivity and the F/C atomic ratio was estimated from the area ratio as described by Equation (3), where A and S represent the peak area and element sensitivity. The extent of fluorine surface segregation was evaluated by the fluorine enrichment factor, calculated with Equation (4).

$$\begin{aligned} \frac{F}{C} \text{ atomic ratio} \\ = \frac{A(F)}{S(F)} / \left(\frac{A(CF_2) + A(CF_3) + A(C=O) + A(C-O) + A(C-C)}{S(C)} \right) \end{aligned} \quad (3)$$

$$\begin{aligned} \text{Fluorine enrichment factor} \\ = \frac{F}{C}(\text{XPS}) / \frac{F}{C}(\text{theoretical bulk average}) \end{aligned} \quad (4)$$

The self-replenishing ability of the UV-cured films was investigated by inflicting an intentional surface damage through

controlled microtoming of thin slices (up to a few tens of μm) in a parallel direction with respect to the original surface of the polymer films. The intended damage was carried out at temperatures close to the T_g of the cured films to minimize the introduction of additional surface roughness by the cutting procedure [33]. Therefore, for films with $T_g < 0$ °C, the microtoming was carried out under cryo-conditions with a Cryostat HM 550 (Microm Systems). The samples with $T_g > 0$ °C were microtomed at room temperature with a Leica RM2165 Microtome. A home-made design sample holder and an epoxy sacrificial layer, as previously reported [33], were used to ensure the removal of surface layers plane-parallel to the films surface and with a minimal introduction of artifacts at the surface, which could affect the post-damage characterization methods. The surface arithmetic roughness (R_a), as obtained with Confocal Optical Microscopy on the films before and after the microtoming only varied slightly, hence, it was assumed that only minor roughness effects were introduced by the microtoming. Details of the microtoming procedures, the use of a sacrificial layer for plane-parallel cuts, and the analyses of the potential roughness or surface defects introduced by the microtoming, are discussed in detail in the Supporting Information (SI, part 4 and Table S1).

3. Results and discussion

3.1. Synthesis of the fluorinated-polymeric dangling chains terminated with a methacrylate group (R_{f8} -PCL₁₆-MA)

The R_{f8} -PCL₁₆-OH dangling chains were synthesized and characterized as described previously [47]. The degree of polymerization (DP) of the PCL-polymeric spacer was chosen as 16, since in the model systems this DP was reported [35] to provide an optimized hydrophobicity of the initial surfaces formed upon thermal-curing. To incorporate a vinyl group into new dangling chains, the terminal OH group was reacted with IEM, following procedures adapted from the literature [20, 21]. From this reaction, dangling chains with a terminal methacrylate group (R_{f8} -PCL₁₆-MA, Fig. 1) were obtained. From the known methacrylate/acrylate copolymerization reactivity ratios [49], it can be inferred that upon radical initiation the dangling chain methacrylate groups will be preferentially built in the network with respect to the acrylate groups of the binder, ensuring that no un-bound R_{f8} chains remain after curing, even at incomplete conversion.

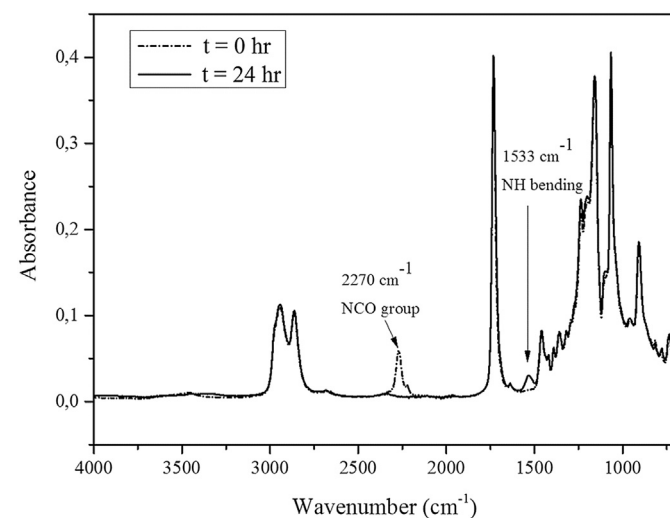


Fig. 2. Conversion the terminal group of the dangling chains from OH- to MA-functionalities: FT-IR ATR spectra of the reaction mixture containing R_{f8} -PCL-OH and IEM, in the beginning of the reaction ($t = 0$) and after 24 h.

The chemical conversion of the IEM isocyanate into a urethane was followed by FT-IR ATR. The consumption of the isocyanate during the reaction was monitored by the disappearance of the vibration band at 2270 cm^{-1} , attributed to the asymmetrical stretching of the $\text{N}=\text{C}=\text{O}$ group (Fig. 2). After 24 h of reaction, this vibration band completely disappeared while a band at 1533 cm^{-1} , attributed to the bending vibration of the $\text{N}-\text{H}$ group of the urethane, appeared with a medium intensity. These observations confirmed the nearly complete conversion of the reactive isocyanate groups and the formation of the urethane bonds under the chosen reaction conditions. Additionally, the presence of a visible vibration band at 1640 cm^{-1} of weak intensity, confirmed the existence of vinyl groups in the reaction product.

The chemical structure of the reaction product was confirmed by ^1H NMR spectroscopy (Fig. 3). In the $\text{R}_{f8}\text{-PCL}_{16}\text{-MA}$ spectra, the peak H_j can be assigned to $-\text{CH}_2$ protons next to the ester group connected to the perfluoroalkyl group. The peak configuration of proton H_k (signal shifted from 3.6 to 3.4) changed from a triplet into a quadruplet, due to the formation of a new coupled proton in the neighboring NH group. The integral ratio of the signals H_k and H_j , $A(\text{H}_k)/A(\text{H}_j)$ is 1, indicating that one molecule of IEM was bonded to one molecule of $\text{R}_{f8}\text{-PCL}_{16}\text{-OH}$. Furthermore, the signals at 6.1 ppm and 5.6 ppm (H_x and H_y , CH_2 protons in the methacrylate group) and at 1.9 ppm (H_m , $-\text{CH}_3$ protons in the methacrylate group) confirm the presence of the vinyl groups of the IEM molecule. Accordingly, the signal of H_z ($-\text{CH}_2$ protons initially next to the OH group) also shifted from 3.5 ppm in the $\text{R}_{f8}\text{-PCL-OH}$ to a higher chemical shift (4.0 ppm in the $\text{R}_{f8}\text{-PCL}_{16}\text{-MA}$). Finally, another signal (H_n) emerged at 6.4 ppm, corresponding to the $-\text{NH}$ in the newly formed urethane bond.

The M_n of the reaction product, as obtained by GPC, showed an increment (from 2744 g/mol for $\text{R}_{f8}\text{-PCL}_{16}\text{-OH}$ to 3073 g/mol for $\text{R}_{f8}\text{-PCL}_{16}\text{-MA}$) which can be attributed to the additional moieties introduced by the IEM molecule; however, the PDI

stayed at 1.18 before and after the modification, indicating no influence on the average molecular weight distribution of the polymeric spacer upon the chemical modification of the end groups of the dangling chains.

3.2. Formation of the hydrophobic polymer films by UV-initiated radical polymerization

For all the polymer films prepared with $\text{R}_{f8}\text{-PCL}_{16}\text{-MA}$, the fluorine content was set at a constant level of 1.5 wt% (weight percentage of fluorine in relation to the total solid content). During the mixing of the monomers and the $\text{R}_{f8}\text{-PCL}_{16}\text{-MA}$, the solutions turned hazy indicating poor miscibility. Therefore, 1,4-dioxane was added at 20 wt% to the mixture to obtain homogeneous solutions. To avoid oxygen inhibition of the radical polymerization [50–52], the polymer films were cured in a N_2 environment.

After UV-curing, tack-free polymer films were obtained for all mixtures prepared. To determine the amount of solvent retained in the polymer films, TGA analyses were performed. The films prepared with the higher molecular weight PEGDA monomers are slightly less thermally stable (Fig. 4), which is explained by the thermal instability of the polyether block as previously reported in the literature [53]. The mass loss at $+101\text{ }^\circ\text{C}$, the boiling temperature of dioxane, was estimated from the thermograms (Fig. 4 and Table 2). For all the films, the mass loss was less than 1.5% in weight which may be attributed to the evaporation of residual dioxane, but also to the moisture absorbed from the atmosphere. The reference polymer films did not contain fluorinated dangling chains, thus no solvent was added. Accordingly, the mass loss observed for the reference films at $+100\text{ }^\circ\text{C}$ corresponds to absorbed moisture only, due to the hydrophilic nature of PEGDA monomer. Since there is almost no difference in mass loss between the reference and the fluorinated-films, this indicates that the majority of the dioxane added to the mixtures had evaporated during the curing process.

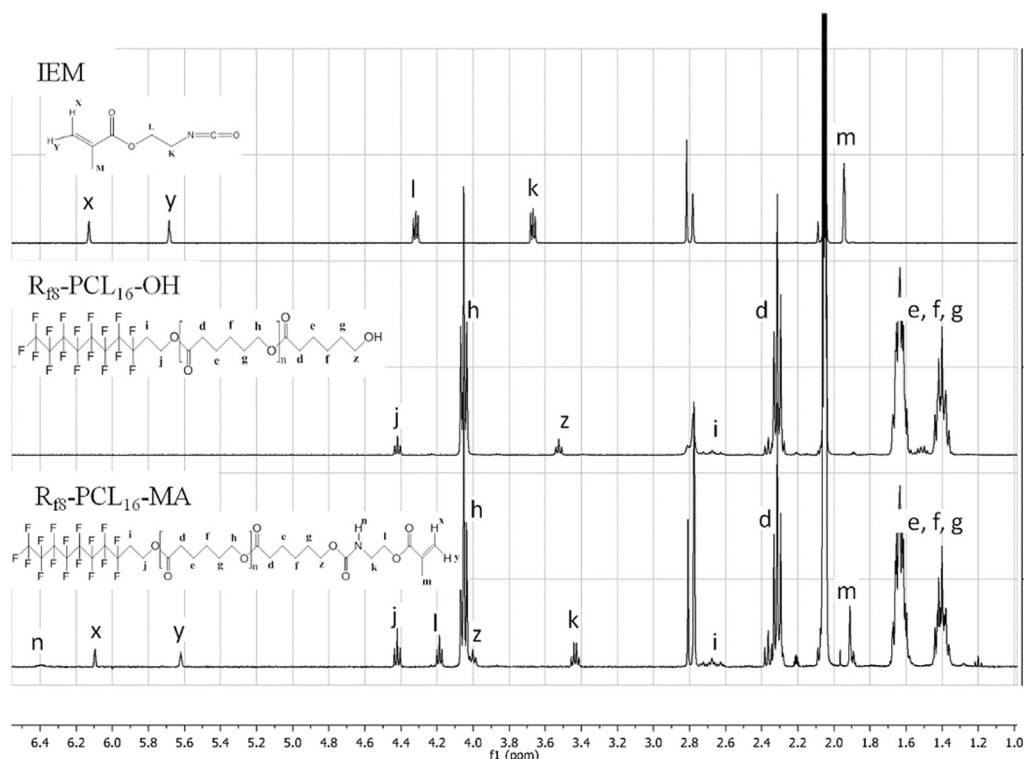


Fig. 3. ^1H NMR spectra of the $\text{R}_{f8}\text{-PCL}_{16}\text{-MA}$ and of the reference reactants, IEM and $\text{R}_{f8}\text{-PCL}_{16}\text{-OH}$.

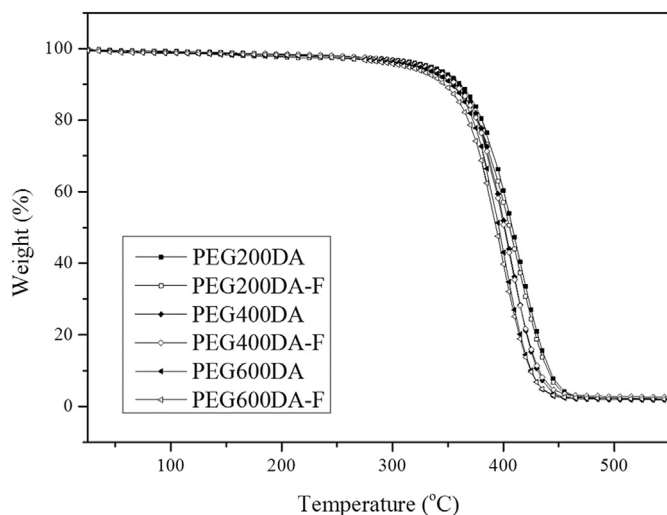


Fig. 4. Thermogravimetric analyses (TGA) of the UV-cured polymer films: solid symbols without and open symbols with R_{18} -PCL-MA.

The T_g 's of the UV-cured polymer films were determined by DSC (Fig. 5). For the reference films, the T_g decreases with increasing M_n of the PEGDA monomer used. This can be explained by the flexibility of $-\text{CH}_2-\text{CH}_2-\text{O}-$ polymer segment. The larger this segment, the softer is the network, i.e., lower T_g . The T_g of the films PEG400DA-F and PEG600DA-F did not differ significantly, as compared to their respective reference films (see Table 2). However, for the PEG200DA-F films a decrease of about 10 °C was observed. The T_g of the R_{18} -PCL₁₆-MA dangling chains is -56 °C which is close to the T_g of the PEG400DA and PEG600DA, but very different from the T_g of the PEG200DA films. Hence, the effect observed for the PEG200DA films is probably due to a plasticizing effect of the presence of R_{18} -PCL₁₆-MA. From Fig. 5 it can also be seen that for the films containing the R_{18} -PCL₁₆-MA dangling chains, a small melting peak appeared around +45 °C, attributed to the crystallization of the PCL-block, formed during cooling. In the first heating run, no such melting peaks were observed (see SI Part 5). The crystallization of the PCL molecules is a well-known phenomenon, dependent on the polymer system characteristics and processing conditions, and has been reported by other authors [54].

The conversion of the vinyl groups of the diacrylate oligomers was investigated by Confocal Raman Microscopy (CRM). For the majority of the films, the peak corresponding to the vinyl bonds was no longer detectable in the Raman spectra after the UV-curing, indicating an almost full conversion of the acrylate/methacrylate groups (Fig. 6A). The only exception was observed for the PEG200DA films, where a very small peak could be identified at 1640 cm^{-1} , attributed to the stretching vibration of the vinyl bonds, and corresponding to a calculated conversion of ~95%. This slightly

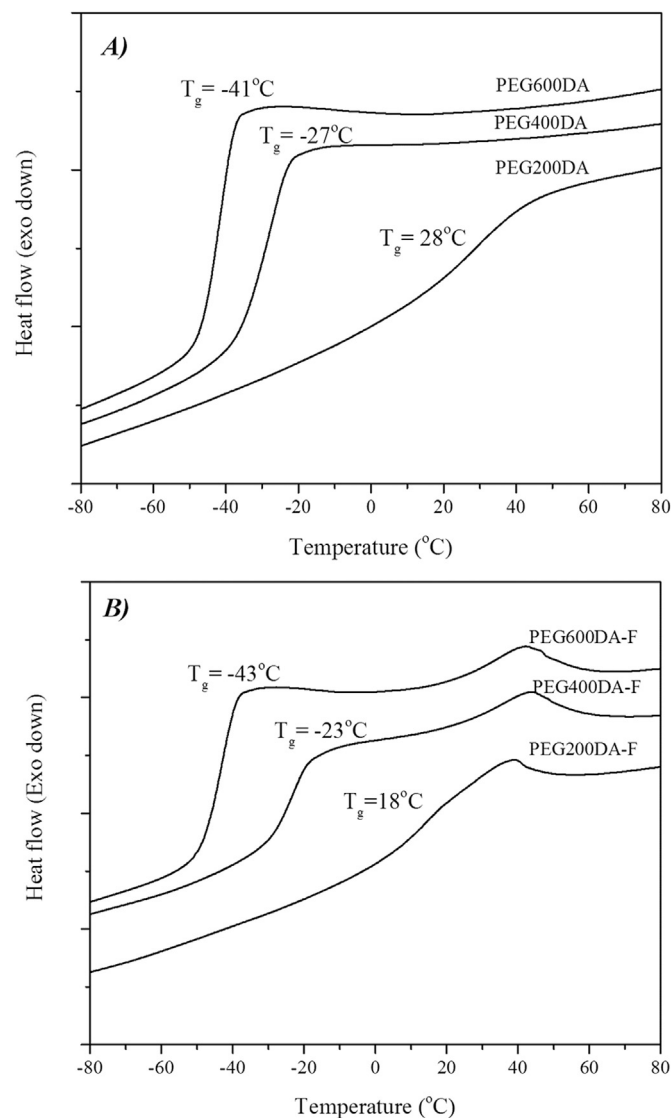


Fig. 5. Differential Scanning Calorimetry (DSC) analyses of the UV-cured films: A) without and B) with R_{18} -PCL-MA. For simplification only the second heating scan is shown.

lower degree of conversion is very likely due to the vitrification effect of PEG200DA with higher T_g , as compared with the other two oligomers. It should be noticed, however, that the effect observed on the oligomer conversion of the PEG200DA films is no longer visible in the PEG200DA-F films (Table 2), which may be due to the plasticizing effect introduced by the additional solvent (dioxane) and the soft dangling chains.

Table 2

Characterization of the UV-cured films: solvent extraction, chemical conversion (CRM), T_g (DSC) and weight loss upon temperature increase (TGA).

	Weight loss after extraction (H_2O) (%)	Weight loss after extraction (CHCl_3) (%)	Chemical conversion (CRM) ^a	T_g (°C) (DSC)	Weight loss at 101 °C (%) (TGA)
PEG200DA	0.6	1.0	95%	+28	0.8
PEG400DA	0.7	1.3	100%	-27	1.2
PEG600DA	0.2	1.1	100%	-41	1.3
PEG200DA-F	0.7	0.7	100%	+18	0.9
PEG400DA-F	0.9	0.8	100%	-23	1.0
PEG600DA-F	0.6	1.9	100%	-43	1.3

^a Calculated based on Equation (4).

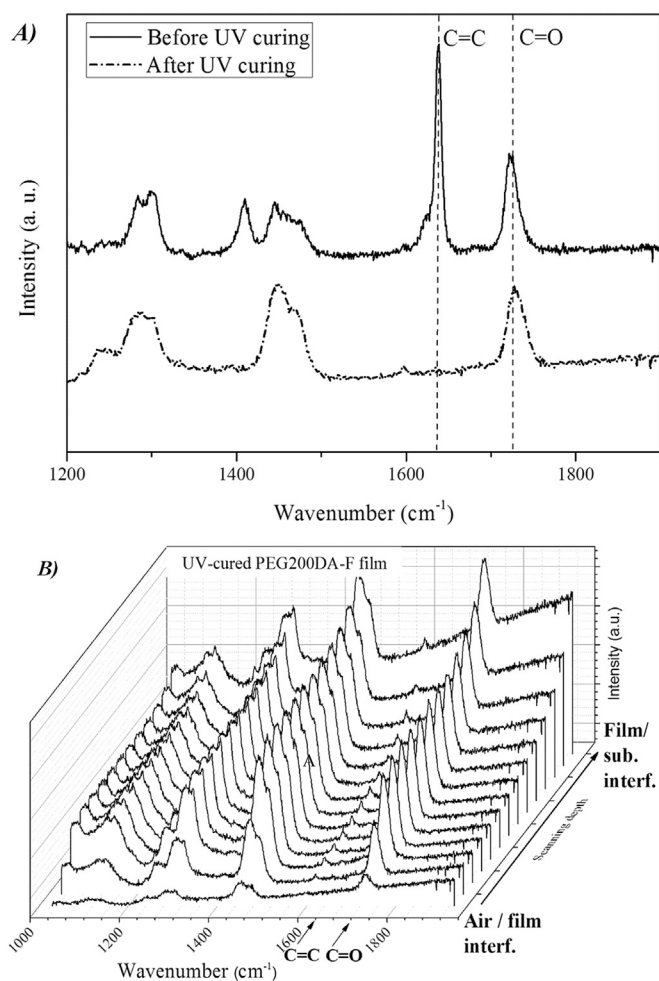


Fig. 6. A) Raman spectra of the PEG200DA-F film top surface before and after the UV curing and B) the depth profile of Raman spectra of the UV-cured PEG200DA-F films.

The conversion of the double bonds at different depths of the UV-cured films was also followed by CRM (Fig. 6B). The absence of the peaks associated to the vinyl bonds across the film strongly suggest an extensive curing throughout the layer, and without oxygen inhibition at the air interface.

The conversion of the methacrylate groups of the R₁₈-PCL₁₆-MA dangling chains, which results in covalent bonding to the polymer network, is of particular relevance. The incorporation of the dangling chains in the polymer networks is crucial for avoiding leaching and for achieving the self-replenishing behavior. From the CRM experiments it was not possible to follow the conversion of the acrylate and methacrylate groups separately, since the vibration bands of the two vinyl bonds fall in the same range (1620–1660 cm⁻¹) and were not

sufficiently resolved [55,56]. Furthermore, the concentration of the acrylate groups was in excess as compared to the methacrylate groups. Hence, to evaluate the amount of un-reacted (or non-network incorporated) dangling chains, solvent extraction procedures were applied to all the UV-cured films. Water, a good solvent for the PEGDA monomers, and chloroform, a good solvent for the PEGDA monomers and R₁₈-PCL₁₆-MA, were used as extracting solvents. For all the UV-cured films the weight loss due to solvent extraction was less than 2 wt% (Table 2). The extractable solid residues were analyzed by ¹H NMR (see SI Part 3). The chemical shifts attributed to the PEGDA-segments and the PCL-blocks (of the fluorinated dangling chains) were identified in the solid residues, but the chemical shifts attributed to the vinyl peaks were absent. These results confirm the high conversions estimated from CRM measurements and indicate that the residues extracted may consist of “free” oligomers, both of PEGDA and of unconnected network residues containing fluorinated dangling chains, as a result of cyclizations and disproportionation side reactions.

The results above show that the networks made by UV-curing of PEGDA monomers in the presence of the R₁₈-PCL₁₆-MA dangling chains were fully cross-linked throughout the depth of the layer, resulting in “tack-free” films with very low percentage of extractable, non-network bonded residues. The full conversion of the double bonds and the absence of vinyl groups in the extractable residues also indicate the successful incorporation of the dangling chains in the polymer networks as required for the self-replenishing behavior (Fig. 1B).

3.3. Surface properties of the UV-cured polymer films

To assess the hydrophobicity of the UV-cured polymer films, dynamic water CA measurements were done. All the reference films prepared without dangling chains showed a water CA_{adv} around 50° (Table 3). The films prepared with the R₁₈-PCL₁₆-MA dangling chains showed a large increase of CA_{adv} and CA_{rec} (Table 3). These results clearly indicated a surface enrichment with the low surface energy (fluorinated) groups of the R₁₈-PCL₁₆-MA dangling chains at the air interface. This enrichment was further confirmed by the Fluorine–Carbon (F/C) atomic ratio calculated from the XPS analyses. Theoretically, if the R₁₈-PCL₁₆-MA incorporated were distributed homogeneously throughout the depth of the polymer films, the F/C atomic ratio at the surface should be equal to the “theoretical bulk average” value, shown in Table 3. In fact, for all the films made with the fluorinated dangling chains, much higher F/C ratios were estimated using XPS (Table 3), indicating surface enrichment factors of 14–20, which explains the significant increase in hydrophobicity.

3.4. Self-replenishing behavior

In previous works on self-replenishing films, thermally cured polyester urethane cross-linked networks were used as model

Table 3
Hydrophobicity of the UV-cured polymer films shown by dynamic (advancing, CA_{adv} and receding, CA_{rec}) water contact angle and surface fluorine-enrichment demonstrated by X-Ray Photoelectron Spectroscopy (XPS).

	CA _{adv} (°)	CA _{rec} (°)	F/C ratio (theoretical bulk average)	F/C ratio (initial surface after UV-curing) (by XPS)	Fluorine enrichment factor
PEG200DA	58 ± 2	34 ± 1	–	–	–
PEG400DA	46 ± 1	32 ± 1	–	–	–
PEG600DA	55 ± 2	36 ± 1	–	–	–
PEG200DA-F	118 ± 2	76 ± 4	0.016	0.225 ± 0.047	14
PEG400DA-F	116 ± 3	87 ± 3	0.016	0.320 ± 0.022	20
PEG600DA-F	114 ± 2	76 ± 6	0.016	0.308 ± 0.008	19

systems. It has been demonstrated that the self-replenishing ability relies on the incorporation of dangling chains which: i) are chemically bonded to the cross-linked network, ii) contain a surface-segregation driving force (e.g., by a low-surface energy “block” consisting of fully fluorinated carbons) and iii) contain a polymeric spacer. These requirements are essential to achieve a good balance between the surface-segregation span mobility and “bulk” miscibility of the dangling chains, which will enable the recovery of the initial surface chemical composition, thus the initial hydrophobicity, on new air-film interfaces created upon the damage.

To study the self-replenishing ability of the current UV-cured polymer films, all the films were submitted to an intentional damage, in which the top layers (of a few to a few tens of μm) were sequentially removed with a microtome, in a parallel direction to the air-film interface. After microtoming the films, the damaged surfaces were characterized from the earliest practical time possible after the damage (≈ 4 h) by dynamic water CA and XPS measurements, to investigate the recovery of hydrophobicity and F/C ratio on the damaged areas, respectively.

The PEG400DA-F and PEG600DA-F films exhibited a high CA_{adv} of $\approx 120^\circ$, which were similar to the CA measured for the original surfaces, after damaging with a short recovery time (≈ 4 h) (Table 4). However, in the same conditions the PEG200DA-F film clearly exhibited a CA_{adv} of 60° and a low CA_{rec} . In comparison to the original values, a significant decrease in CA_{rec} was observed for all the films upon damage, which may be attributed to the enhanced surface roughness introduced by the microtoming (SI Part 4). It has been described that the CA_{rec} measurements can be easily influenced by liquid sorption/retention and penetration [57] into surfaces, which can be significantly enhanced by additional surface roughness.

All the intentionally damaged UV-cured films were then allowed to recover for 2 days at room temperature inside a desiccator. After this period, the PEG400DA-F and PEG600DA-F films showed the same water contact angles as before (after 4 h of recovery) but surprisingly, the PEG200DA-F film also exhibited a rather high CA_{adv} and a higher CA_{rec} (Table 4), closer to the original surface water CA values (Table 3). These results clearly show that surface hydrophobicity can be reestablished for all the three UV-cured films to a large extent, albeit with different recovery time. The intentionally damaged surfaces were also characterized by XPS to determine the F/C atomic ratio after 2 days, by analyzing the polymer layers removed sequentially at different cutting depths (Fig. 7). For all the films and at all cutting depths, the F/C atomic ratio was significantly higher than the “theoretical bulk average” (Table 3 and dashed line in Fig. 7), with surface enrichment factors between 14 and 20. Furthermore, these values were maintained, within the error margins, at the same level of the respective original surfaces. These results clearly indicate that after damage and recovery, the new air-interfaces of the films are replenished with fluorinated dangling chains, which explains the recovery of their hydrophobicity after damage.

Table 4

Dynamic (advancing, CA_{adv} and receding, CA_{rec}) water contact angles measured on polymer films, on the original surfaces and on surfaces created after intentional damage (by microtoming), 4 h and 2 days of recovery (at room temperature and inside an desiccator).

	Initial		4 h of recovery		2 days of recovery	
	CA_{adv} ($^\circ$)	CA_{rec} ($^\circ$)	CA_{adv} ($^\circ$)	CA_{rec} ($^\circ$)	CA_{adv} ($^\circ$)	CA_{rec} ($^\circ$)
PEG200DA-F	118 ± 2	76 ± 4	60 ± 2	11 ± 4	118 ± 1	47 ± 4
PEG400DA-F	116 ± 3	87 ± 3	120 ± 1	61 ± 1	121 ± 1	59 ± 3
PEG600DA-F	114 ± 2	76 ± 6	119 ± 1	44 ± 3	121 ± 1	46 ± 2

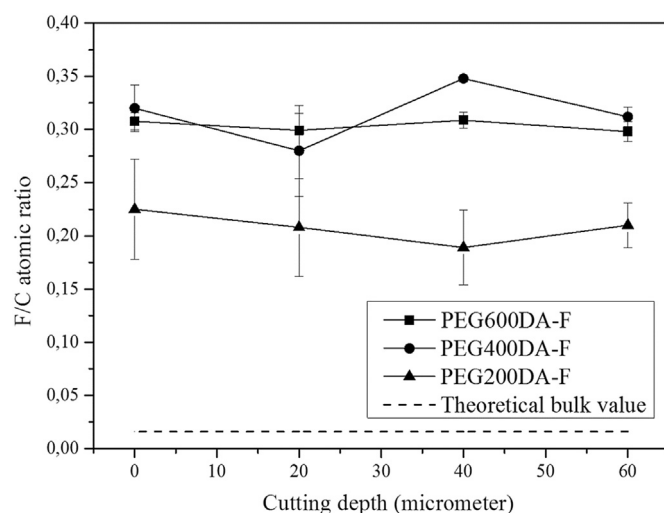


Fig. 7. Fluorine/Carbon (F/C) atomic ratio, determined by XPS, for the UV-cured films containing R_{18} -PCL-MA dangling chains, at different depths of the films (assessed upon microtoming of layers parallel to the air-polymer interface). Cutting depth = 0 μm corresponds to the original, non-damaged surfaces. Dashed line corresponds to the “theoretical bulk value” expected, if the dangling chains were homogeneously distributed throughout the “bulk” of the polymer film, i.e., no surface segregation.

3.5. UV-cured polymer networks and PEG-segment length effect

In spite of the fact that the network formation of the UV-cured acrylate-based films occurs much faster than in the thermally cured model systems [35], the results obtained clearly show that the films exhibit a self-replenishing behavior with a healing efficiency of nearly 100%.

It is interesting to notice that all the original films containing the R_{18} -PCL₁₆-MA dangling chains were very hydrophobic ($CA_{adv} \approx 114$ – 118° , Table 3). This is a clear indication that the fast curing process (only 30 s of UV-irradiation) did not restrict the initial surface-segregation and allowed for sufficient fluorinated dangling chains to be positioned at the air-interface, resulting in high water CA. The use of a polymeric spacer (PCL) (Fig. 1B) and of a small amount of solvent (dioxane) to enhance the miscibility/mobility of the dangling chains may have been crucial to allow a sufficient surface-enrichment during film formation.

Although the water CA on the original surfaces did not seem to be influenced by the PEG-block length, the F/C atomic ratios investigated by XPS clearly show an effect (Table 3). The “softer” films, PEG400DA-F and PEG600DA-F (Table 2), have a higher F/C atomic ratio, as compared to the more “rigid” PEG200DA-F films (Table 3). Considering that all films have the same low level of extractable solid residues, they must contain similar amount of dangling chains incorporated (Table 2). Judging from the high CA and the enrichment factors (Table 3), a considerable fraction of the incorporated fluorinated dangling chains is expected to be positioned at the top-surface (i.e., air-polymer interface). This particular fraction of dangling chains is covalently bonded to the network but has enough mobility and span to reach the surface, hence, will not be strongly affected by differences in the network characteristics, given sufficient mobility. However, the fluorinated dangling chains positioned in the immediate sub-surface and in the layers below, will not have enough span to reach the top-surface. Hence, their positioning and orientation in the network will be affected by the network characteristics, namely different architectures created upon acrylic-based free radical UV-curing processes. This may explain the differences observed for the F/C atomic ratio on the

fluorinated-PEGDA films within the probed film depth. It should be noted that XPS characterization provides the composition within the top ≈ 10 nm layer from the air-interface inwards. A fully stretched fluorinated C_8F_{17} group is ≈ 1 nm and C_8F_{17} -PCL-OH chain is about ≈ 5 nm. Hence, the difference in F/C atomic ratios estimated using XPS could be due to different occurrence/positioning of dangling chains within the top 10 nm of the films, which comprises the top- and sub-surface layers.

In spite of the lower F/C atomic ratio observed for the original surface of the PEG200DA-F films, the F/C atomic ratio measured on sliced polymer layers (after 2 days of recovery) was constant (within the error margins) throughout different cutting depths (up to 60 μm) indicating a multiple self-replenishing ability (Fig. 7). The same multiple-healing ability was observed for the “softer” films, PEG400DA-F and PEG600DA-F. Hence, these results clearly show that for all the films prepared, the fast curing of the acrylate-based network did not hinder the successful incorporation of the dangling chains into the network during film formation, and that a good balance between chemical bonding and the initial surface segregation was achieved.

The time-periods involved in the surface recovery were very clearly affected by the segment length of the PEGDA monomers used. Films with “softer” network segments (PEG400DA and PEG600DA) reached the maximum of the hydrophobicity recovery within 4 h, while the films with more “rigid” network segments (PEG200DA) still showed hydrophilic properties (Table 4) in that time frame. After 2 days of recovery all the films showed water CA and F/C ratios similar to the values measured on non-damaged films.

For the PEG200DA films in particular, we measured the F/C ratio on layers of the coating microtomed at different depths throughout the bulk of the film, after being kept at room temperature and inside and exsiccator for different time periods, see Fig. 8. From these results it is clear that the F-content gradually recovers, from 4 h up to 2 days after the damage, to the F/C ratio of the original coating (shown at $\mu\text{m} = 0$ in Fig. 8). Accordingly, the hydrophobicity was also recovered spontaneously, moreless within the same time-interval, see dynamic water CA in Table 5. These results clearly eliminate any speculation that the constant F-content level at various cutting depths throughout the bulk, observed after 2 days

Table 5

Dynamic (advancing, CA_{adv} and receding, CA_{rec}) water contact angles measured on PEG200DA-F films, at different times of recovery (hours) after damage. The original surfaces and the surfaces created after intentional damage (by microtoming) were left for the different times measured, at room temperature and inside an desiccator.

Time of recovery (hours)	CA_{adv} ($^\circ$)	CA_{rec} ($^\circ$)
0	118 ± 2	76 ± 4
4	62 ± 2	20 ± 2
24	98 ± 4	40 ± 4
48	118 ± 1	47 ± 4

for all the samples (shown in Fig. 7), could be due to F-contamination by microtoming procedure. It should be noted that the T_g of the “softer” films is far below room temperature (RT) (Fig. 5 and Table S1) while for these PEG200DA-F films it is around $+18$ $^\circ\text{C}$. This could explain why in the latter case the re-orientation of the dangling chains towards the new surfaces created upon damage, takes a longer time to achieve a maximum of self-replenishing of nearly 100%.

4. Conclusions

Low surface energy polymeric dangling chains consisting of perfluoroalkyl-end capped linear polymeric spacers (PCL-based) with a terminal methacrylate group were successfully synthesized. These dangling chains were incorporated into PEGDA-based cross-linked polymer networks via UV-initiated radical polymerization. The surface hydrophobicity of the films with the fluorinated-dangling chains was strongly increased. After the intentional damaging, the rate of hydrophobicity recovery was found to be dependent on the networks properties (such as T_g), which is associated with the PEG segment length of the PEGDA monomers used. Despite clear differences in the speed of network formation as compared with previously reported systems, all the UV-cured polymer films exhibit a clear, multiple self-replenishing ability, and recovered the initial chemical composition and hydrophobicity, at air-polymer interfaces created after surface damages. These new self-replenishing acrylate-based systems, cured by a faster and more eco-friendly process, are one step closer to the application of hydrophobic polymer films with a surface functionality self-repairing ability, in areas like automotive or aerospace engineering, where functionalities like self-cleaning/easy-to-clean are highly desired. Currently we are also investigating alternatives to achieve similar self-replenishing behavior on low surface energy films using more eco-friendly chemistries, namely silicon-based components as an alternative to F-components, which will be reported in a follow-up publication.

Acknowledgment

This research forms part of the research program of the Dutch Polymer Institute (DPI), project #758 (SER-LED).

Appendix A. Supplementary data

Supplementary data related to this article can be found at <http://dx.doi.org/10.1016/j.polymer.2015.02.036>.

References

- [1] Zeiler T, Kellermann S, Munstedt H. *J Adhes Sci Technol* 2000;14:619–34.
- [2] Wheale SH, Badyal JPS. *Polymer* 2011;52:5250–4.
- [3] Emoto K, Nagasaki Y, Iijima M, Kato M, Kataoka K. *Colloid Surf B* 2000;18:337–46.
- [4] Granville AM, Boyes SG, Akgun B, Foster MD, Brittain WJ. *Macromolecules* 2005;38:3263–70.

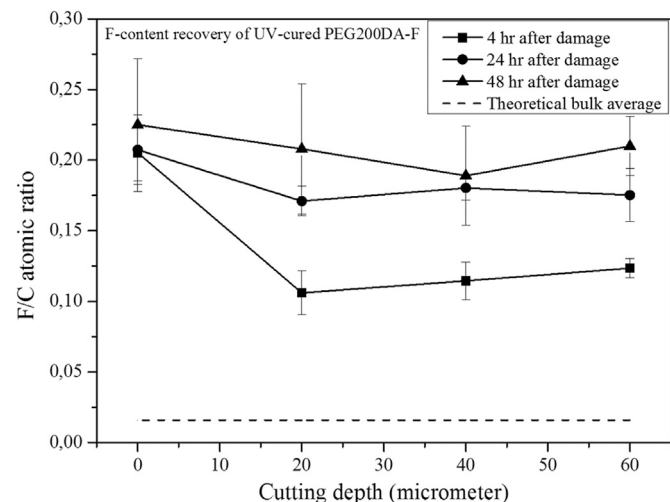


Fig. 8. Fluorine/Carbon (F/C) atomic ratio, determined from XPS at different times of recovery after the damage, for the UV-cured PEG200DA-F film containing Rf8-PCL-MA dangling chains, at different depths of the films (assessed upon microtoming of layers parallel to the air-polymer interface). Cutting depth = 0 μm corresponds to the original, non-damaged surfaces. Dashed line corresponds to the “theoretical bulk value”.

- [5] Rohr T, Ogletree DF, Svec F, Frechet JM. *Adv Funct Mater* 2003;13:264–70.
- [6] Durand N, Gaveau P, Silly G, Ameduri B, Boutevin B. *Macromolecules* 2011;44:6249–57.
- [7] Majumdar P, Webster DC. *Polymer* 2007;48:7499–509.
- [8] Majumdar P, Webster DC. *Polymer* 2006;47:4172–81.
- [9] Bongiovanni R, Malucelli G, Messori M, Pilati F, Priola A, Tonelli C, et al. *J Polym Sci Pol Chem* 2005;43:3588–99.
- [10] Mielczarski JA, Mielczarski E, Galli G, Morelli A, Martinelli E, Chiellini E. *Langmuir* 2010;26:2871–6.
- [11] Martinelli E, Sarvothaman MK, Alderighi M, Galli G, Mielczarski E, Mielczarski JA. *J Polym Sci Pol Chem* 2012;50:2677–86.
- [12] Thomas RR, Anton DR, Graham WF, Darmon MJ, Stika KM. *Macromolecules* 1998;31:4595–604.
- [13] Pike JK, Ho T, Wynne KJ. *Chem Mater* 1996;8:856–60.
- [14] Ming W, Ravenstein Lv, Grampel Rvd, Gennip Wv, Krupers M, Niemantsverdriet H, et al. *Polym Bull* 2001;47.
- [15] Ming W, Melis F, van de Grampel RD, van Ravenstein L, Tian M, van der Linde R. *Prog Org Coat* 2003;48:316–21.
- [16] Carr C, Wallstom E. *Prog Org Coat* 1996;28:161–71.
- [17] van de Grampel RD, Ming W, van Gennip WJH, van der Velden F, Laven J, Niemantsverdriet JW, et al. *Polymer* 2005;46:10531–7.
- [18] O'Rourke-Muisener PAV, Koberstein JT, Kumar S. *Macromolecules* 2003;36:771–81.
- [19] Koberstein JT. *J Polym Sci Pol Phys* 2004;42:2942–56.
- [20] Wong DA, O'Rourke-Muisener PAV, Koberstein JT. *Macromolecules* 2007;40:1604–14.
- [21] Thompson RL, Narrainen AP, Eggleston SM, Ansari IA, Hutchings LR, Clarke N. *J Appl Polym Sci* 2007;105:623–8.
- [22] Hutchings LR, Narrainen AP, Eggleston SM, Clarke N, Thompson RL. *Polymer* 2006;47:8116–22.
- [23] Toohey KS, Sottos NR, Lewis JA, Moore JS, White SR. *Nat Mater* 2007;6:581–5.
- [24] Hager MD, Greil P, Leyens C, van der Zwaag S, Schubert US. *Adv Mater* 2010;22:5424–30.
- [25] Garcia SJ, Fischer HR, van der Zwaag S. *Prog Org Coat* 2011;72:211–21.
- [26] White SR, Sottos NR, Geubelle PH, Moore JS, Kessler MR, Sriram SR, et al. *Nature* 2001;409:794–7.
- [27] Blaiszik BJ, Sottos NR, White SR. *Compos Sci Technol* 2008;68:978–86.
- [28] Lafont U, van Zeijl H, van der Zwaag S. *ACS Appl Mater Inter* 2012;4:6280–8.
- [29] Varley RJ, van der Zwaag S. *Acta Mater* 2008;56:5737–50.
- [30] Wietor JL, Dimopoulos A, Govaert LE, van Benthem RATM, de With G, Sijbesma RP. *Macromolecules* 2009;42:6640–6.
- [31] Pepels M, Filot I, Klumperman B, Goossens H. *Polym Chem-Uk* 2013;4:4955–65.
- [32] Rodriguez ED, Luo XF, Mather PT. *ACS Appl Mater Inter* 2011;3:152–61.
- [33] Dikić T, Ming W, van Benthem RATM, Esteves ACC, de With G. *Adv Mater* 2012;24:3701–4.
- [34] Esteves ACC, Lyakhova K, van Riel JM, van der Ven LGJ, van Benthem RATM, de With G. *J Chem Phys* 2014;140.
- [35] Esteves ACC, Lyakhova K, van der Ven LGJ, van Benthem RATM, de With G. *Macromolecules* 2013;46:1993–2002.
- [36] Lyakhova K, Esteves ACC, van de Put MWP, van der Ven LGJ, van Benthem RATM, de With G. *Adv Mater Interf* 2014;1:1400053–63.
- [37] Esteves ACC, Luo Y, van de Put MWP, Carcouët CCM, de With G. *Adv Funct Mater* 2014;24:986–92.
- [38] Li Y, Li L, Sun JG. *Angew Chem Int Ed* 2010;49:6129–33.
- [39] Jin H, Tian XL, Ikkala O, Ras RHA. *ACS Appl Mater Inter* 2013;5:485–8.
- [40] Wang HD, Zhou H, Gestos A, Fang J, Lin T. *ACS Appl Mater Inter* 2013;5:10221–6.
- [41] Wang HX, Xue YH, Ding J, Feng LF, Wang XG, Lin T. *Angew Chem Int Ed* 2011;50:11433–6.
- [42] Kuroki H, Tokarev I, Nykypanchuk D, Zhulina E, Minko S. *Adv Funct Mater* 2013;23:4593–600.
- [43] Bongiovanni R, Montefusco F, Priola A, Macchioni N, Lazzeri S, Sozzi L, et al. *Prog Org Coat* 2002;45:359–63.
- [44] Ameduri B, Bongiovanni R, Malucelli G, Pollicino A, Priola A. *J Polym Sci Pol Chem* 1999;37:77–87.
- [45] Gan Y, Yin J, Jiang X. *J Mater Chem A* 2014;2:18574–82.
- [46] Studer K, Decker C, Beck E, Schwalm R. *Eur Polym J* 2005;41:157–67.
- [47] Dikić T, Ming W, Thüne PC, van Benthem RATM, de With G. *Polym Sci Pol Chem* 2008;46:218–27.
- [48] Froud CA, Hayward IP, Laven J. *Appl Spectrosc* 2003;57:1468–74.
- [49] Roos SG, Muller AHE, Matyjaszewski K. *Macromolecules* 1999;32:8331–5.
- [50] Courtecuisse F, Cerezo J, Croutxé-Barghorn C, Dietlin C, Allonas X. *J Polym Sci Pol Chem* 2013;51:635–43.
- [51] Belon C, Allonas X, Croutxé-Barghorn C, Lalevee J. *J Polym Sci Pol Chem* 2010;48:2462–9.
- [52] Courtecuisse F, Belbakra A, Croutxé-Barghorn C, Allonas X, Dietlin C. *J Polym Sci Pol Chem* 2011;49:5169–75.
- [53] Grassie N, Mendoza GAP. *Polym Degrad Stabil* 1984;9:155–65.
- [54] Lee KM, Knight PT, Chung T, Mather PT. *Macromolecules* 2008;41:4730–8.
- [55] Schrof W, Beck E, Koniger R, Reich W, Schwalm R. *Prog Org Coat* 1999;35:197–204.
- [56] van den Brink M, van Herk AM, German AL. *Process Contr Qual* 1999;11:265–75.
- [57] Lam CNC, Wu R, Li D, Hair ML, Neumann AW. *Adv Colloid Interfac* 2002;96:169–91.